Front. Energy 2021, 15(4): 810–831
https://doi.org/10.1007/s11708-021-0760-1

FEATURE ARTICLE

Long GU, Xingkang SU

Latest research progress for LBE coolant reactor of China initiative accelerator driven system project

Abstract China's accelerator driven subcritical system (ADS) development has made significant progress during the past decade. With the successful construction and operation of the international prototype of ADS superconducting proton linac, the lead-based critical/subcritical zero-power facility VENUS-II and the comprehensive thermal-hydraulic and material test facilities for LBE (lead bismuth eutectic) coolant, China is playing a pivotal role in advanced steady-state operations toward the next step, the ADS project. The China initiative Accelerator Driven System (CiADS) is the next facility for China's ADS program, aimed to bridge the gaps between the ADS experiment and the LBE cooled subcritical reactor. The total power of the CiADS will reach 10 MW. The CiADS engineering design was approved by Chinese government in 2018. Since then, the CiADS project has been fully transferred to the construction application stage. The subcritical reactor is an important part of the whole CiADS project. Currently, a pool-type LBE cooled fast reactor is chosen as the subcritical reactor of the CiADS. Physical and thermal experiments and software development for LBE coolant were conducted simultaneously to support the design and construction of the CiADS LBE-cooled subcritical reactor. Therefore, it is necessary to introduce the efforts made in China in the LBE-cooled fast reactor to provide certain supporting data and reference solutions for further design and development for ADS. Thus, the roadmap of China's ADS, the development process of the CiADS, the important design of the current CiADS subcritical reactor, and the efforts to build the LBE-cooled fast reactor are presented.

Keywords LBE (lead bismuth eutectic) coolant reactor, China initiative Accelerator Driven System (CiADS) project, research progress

Received Nov. 25, 2020; accepted Mar. 6, 2021; online Jul. 25, 2021

Long GU (✉)
Institute of Modern Physics, Chinese Academy of Sciences, Lanzhou 730000, China; School of Nuclear Science and Technology, University of Chinese Academy of Sciences, Beijing 100049, China; School of Nuclear Science and Technology, Lanzhou University, Lanzhou 730000, China
E-mail: gulong@impcas.ac.cn

Xingkang SU
Institute of Modern Physics, Chinese Academy of Sciences, Lanzhou 730000, China; School of Nuclear Science and Technology, University of Chinese Academy of Sciences, Beijing 100049, China

Special Issue: Innovative Nuclear Energy Technology

1 Introduction

The rapid progress of human civilization and socio-economic development has been supported by traditional fossil fuels since the 19th century. However, with the massive extraction and use of fossil fuels, fossil energy shortages and environmental pollution have evolved into two of the most critical issues facing humanity in the 21st century. Thus, the development of green energy has become a priority for the global world. Nuclear power has outstanding advantages in high efficiency, reliability, and low carbon emissions. It is considered as a strategic choice to solve the future energy supply and ensure sustainable economic and social development [1,2]. However, it is important to solve two major issues addressed while ensuring the sustainable development of nuclear power: the stable and reliable supply of nuclear fuel resources and the safe disposal of spent nuclear fuel.

The advanced nuclear fuel cycle of the "partitioning-transmutation" concept was suggested in the 1990s to solve the problem of safe disposal of spent nuclear fuel [3–6]. The accelerator driven subcritical system (ADS) drives subcritical reactors to transmute long-lived radioactive nuclides into short-lived or stable nuclides by bombarding the heavy atomic nuclei with high-energy and high-intensity proton beam provided by the accelerator to produce high-throughput and broad-spectrum spallation neutrons. The ADS is considered as the most promising transmutation facility to solve safe disposal of the minor

actinides (MAs) in the future [7–14]. The Nobel Price owned professor C. Rubbia has proposed the European EUROTRANS program [4] since 1986 to promote the ADS technology in the future. Ever since then, many countries have paid great attention to the ADS technology and established many plans to develop this prototype facility [15–26]. For more than 30 years, much excellent work has been accomplished for the high-power linac and lead-cooled fast reactor (LFR). However, the integrated ADS facility has not been built until now. Currently, the Belgian Nuclear Research Centre has been committed to the long-term development of MYRRHA (Multi-purpose hybrid research reactor for high-tech applications), which is the world's first large-scale ADS that consists of an LFR that can operate in both critical and subcritical dual-modes driven by a high-power linear accelerator. The MYRRHA is scheduled to be commissioned in 2036 [27,28]. The China initiative Accelerator Driven System (CiADS) is also devoted to establishing an experimental and verification ADS facility globally [29–31]. It is necessary to report China's practices and efforts in the ADS project. The overview of the CiADS project and the latest research progress for the LBE coolant reactor of the CiADS project are presented in this paper.

2 ADS research development history and roadmap in China

China initiated its study of the ADS technology in the mid-1990s [32]. With the support of the China National Nuclear Corporation (CNNC), the ADS concept research group was established to study the physical feasibility of the ADS system [33]. In 1996, the ADS concept was first introduced into China's nuclear community by professor Guangxi Dai from the Institute of Modern Physics of the Chinese Academy of Sciences (IMPCAS) [34]. Subsequently, China's ADS research was supported by the National Natural Science Project in 1999 and 2007, respectively [35–37]. Under the guidance of Academicians Dazhao Ding, Shouxian Fang, and other scientists, a series of achievements were made in technology exploration and research on various subsystems of ADS.

After a comprehensive and in-depth gestation and condensation from 2009 to 2010, the roadmap for developing ADS in China has been proposed by Chinese Acadeny of Sciences (CAS), based on the significant needs for the sustainable development of China's nuclear energy. The roadmap is divided into three phases. The first phase is the proof-of-principle phase, in which the accelerator-driven transmutation verification research facility will be built around 2024. The second phase is the industrial demonstration phase, in which the accelerator-driven transmutation demonstration facility will be created. The third phase is the industrial application phase, in which the accelerator-driven transmutation system will be scaled up to the GW_{th} magnitude.

During 2011–2016, the strategic pilot project "Future Advanced Fission Energy — ADS Transmutation Systems" was launched by CAS, which is also led by the IMPCAS, focusing on solving individual vital technical problems in the ADS system. Three vital technological breakthroughs were made, including accomplishment of the goal of making the continuous beam current and the pulse beam of the prototype of China's ADS superconducting proton linac reach 26.1 MeV/12.6 mA and 25 MeV/0.17 mA, respectively; the accomplishment of China's lead-based critical/subcritical zero-power facility for ADS research; and the establishment of the comprehensive thermal-hydraulic and material test facility for LBE coolant [32].

The Chinese government has decided to support IMPCAS in leading the design and construction of the integrated ADS project, the so-called CiADS backed by the national primary science and technology infrastructure project of the "12th Five-Year Plan" [38,39].

3 Development route of the CiADS project

In December 2015, the establishment of the CiADS project was officially approved by the National Development and Reform Commission (NDRC). The CiADS will be constructed in Huizhou, Guangdong province [40]. The exceptional foundation for the infrastructure construction was supported by Guangdong province in December 2017. In January 2018, the Feasibility Study Report of the CiADS with a six-year construction period was approved by the NDRC. The "Environmental Impact Report on the CiADS project (site selection stage)" was approved by the Ministry of Ecology and Environment in May 2018. In June 2018, the Preliminary Design Report of the CiADS project was approved by the CAS. The "Site Safety Analysis Report of the CiADS project" was also approved by the National Nuclear Safety Administration in July 2018 [41]. Since then, the CiADS project has been fully transferred to the construction application stage. Because of the lack of construction foundation and technical adjustment, the Feasibility Study Adjustment Report of the CiADS project was submitted to the NDRC and approved in July, 2020. Thus, the CiADS project has been fully approved by the national government. The CiADS installation area and plant site are shown in Fig. 1.

Figure 2 demonstrates the layout of the CiADS. There are five different terminals numbered from T1 to T5 in the CiADS. T1 is the terminal to study and verify the ADS concept and integrate the accelerator and the subcritical reactor. T2 is used for studying hot tests of high-power spallation target and advanced target technology. T3 is to collect high-power beam and irradiation nuclear materials. T4 is adopted to study the reliability of the ADS accelerator and obtain the nuclear database of the ADS. T5 is a reserved

(a) (b)

Fig. 1 Schematic diagram of CiADS project.
(a) Installation area; (b) plant site.

terminal for studying rare isotope and ADS fuel based on the accelerator and the coupling of the small experimental reactor. The design mainly tests the safety characters for the CiADS project and verifies key nuclear safety issues for the ADS facility. The accelerator is approximately 300 m long and the reactor is about 60 m high.

Table 1 summarizes the main design parameters of the CiADS project. The total power of the CiADS is 10 MW, including the power of the subcritical reactor and proton beam. The superconducting linac technology with 500 MeV/5 mA and the LBE-cooled subcritical reactor with a maximum power of 10 MW have been chosen for the CiADS project. There are two operation modes for the accelerator: continuous wave (CW) and pulse operation modes. The CW mode is used for the normal power operation, and the pluse mode is used for reactor physics measurement. In Table 1, the operation value is a little bit smaller compared to the design value because the design value must take into consideration every operation condition in the beginning.

4 Latest design of subcritical reactor of CiADS

4.1 Overall design

Benefiting from the advantages of the LBE with a good

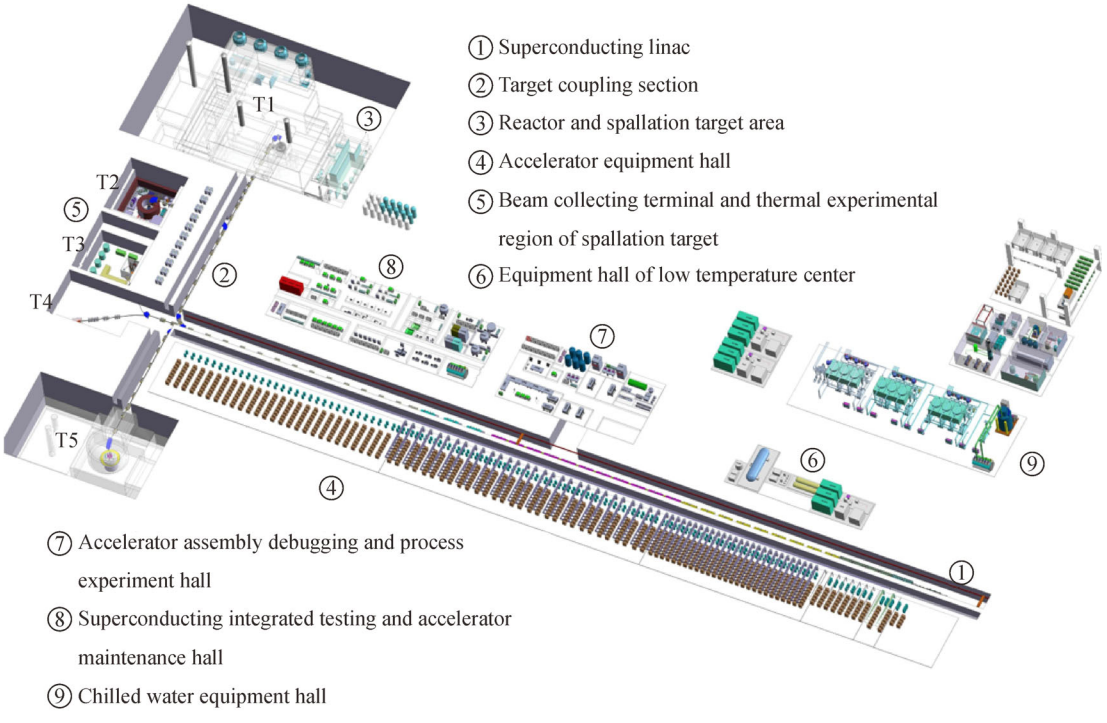

Fig. 2 Layout of CiADS.

Table 1 Overall design parameters of CiADS

	Parameter	Design value	Operation value
CiADS	Total power (reactor + beam)/MW	10	10
	Full power operation time/a	3	⩽3
	Annual operation time/month	3	⩽3
Superconducting linac	Accelerating particles	Proton	Proton
	Energy/MeV	500	500
	Maximum beam power/MW	2.5	2.26
	Operation mode	CW/pulse	CW/pulse
High power spallation target	Maximum bearable beam power/MW	2.5	2.26
Subcritical reactor	Energy spectrum	Fast neutron	Fast neutron
	Maximum thermal power/MW	10	9.76

thermal-hydraulic performance, high boiling point, and low chemical inertness, a pool-type LBE cooled fast reactor is chosen as the subcritical reactor of the CiADS. Figure 3 illustrates the main layout of the primary coolant system, including nuclear assemblies, the core internal structure, an inner barrel, a reactor vessel and a vessel head, four primary heat exchangers, two primary pumps, a fuel elevating and handling machine, and a rotating plug. The main design parameters of the CiADS subcritical reactor are listed in Table 2. In normal operation, the LBE forced circulation driven by the main pump is used for heat export. Under accident conditions, the physical properties of the LBE are fully utilized to enhance the natural circulation capacity of the subcritical reactor. The natural convection between the auxiliary heat exchanger and the core is used to derive the residual heat.

The LBE coolant absorbs the fission energy, transfers the heat to the primary heat exchangers, and then is pumped into the bottom of the reactor core. In this process, the temperature of the LBE coolant is changed from 280°C to 380°C. The CiADS subcritical reactor is not used for the generation of electricity. Thus, the molten salt (ternary nitrates) is used for the secondary coolant to maintain the heat balance between the primary and secondary loop. Considering the static pressure of the LBE coolant in the reactor core, both the primary loop pressure and secondary loop pressure are set to 0.1 MPa. The inlet and outlet temperatures of the secondary system are 220°C and 230°C, respectively. If high-pressure water is used as the secondary coolant, the high-pressure cooling water in the secondary circuit will be injected into the primary coolant through the break when the heat exchanger pipe breaks. Once the high-pressure cooling water is in direct contact with LBE of low pressure and high temperature, a pressure

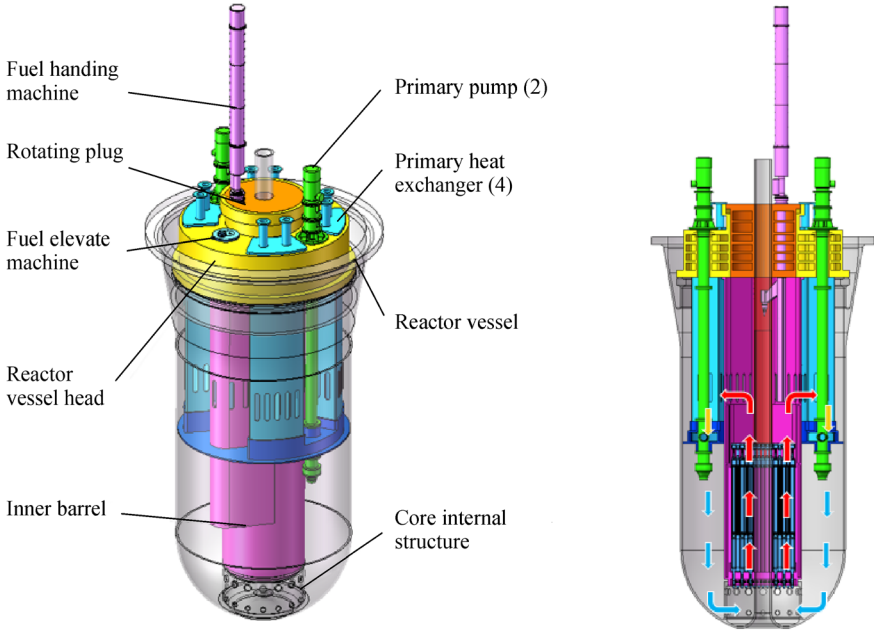

Fig. 3 Layout of LBE cooled subcritical reactor of CiADS.

Table 2 Overview of main technical parameters of CiADS subcritical reactor

Characteristic	Value or description
Reactor type	LBE-cooled fast reactor
Thermal capacity/MW_{th}	10
Fuel composition and ^{235}U enrichment	UO_2 (19.75 wt%)
Primary system	Pool-type
Primary circulation	Forced
Primary coolant	LBE
Primary system pressure/MPa	0.1
Primary system temperature/°C	280–380
Number of primary heat exchanger	4
Primary pump	Mechanical pump × 2
Secondary coolant	Molten salt (Ternary Nitrates)
Secondary system pressure/MPa	0.1
Secondary system temperature/°C	220–230

wave will be released. The subsequent pressure evolution and steam propagation will occur, threatening the integrity of the core structure [42]. Due to the advantages of low pressure and high boiling point of molten salt, the risk of the heat exchanger tube rupture (HXTR) caused by high-pressure water can be avoided.

4.2 Design of LBE subcritical reactor

The layout of the subcritical reactor core is exhibited in Fig. 4. The blue part will be used to place the fuel assemblies. The blue one with a green hole will be used as irradiation channels for the ADS experiment. The green one refers to the reflector assembly, and the green one with a black hole inside represents a replaceable reflector assembly. The red one illustrates the shielding assembly. The CiADS is a system for ADS experiments. Different reactor core schemes are needed for different experiments. Thus, the location of the fuel assembly replacement in the reactor, that is, the white part in Fig. 4, is used to arrange the redundant fuel assembly when the experimental scheme is switched.

In regular operation, the effective multiplication factor k_{eff} of the reactor is nearly 0.975. Fifty-two assemblies with 19.75% of enrichment UO_2 are used in this design and provide thermal power of approximately 9.76 MW. The core design specifications of the CiADS are tabulated in Table 3. The average linear power density of a fuel rod is 1885 W/cm.

In Fig. 5, the regular hexagonal fuel assembly is adopted into the CiADS subcritical reactor. Each fuel assembly has 162 fuel rods and 7 guide tubes. The fuel rods are separated by quincunx grid elements, and the quincunx grid is fixed on guide tubes by spot welding. The special design for this assembly is that additional weight against the buoyancy force of LBE and locking mechanisms are considered.

It is necessary to consider the thermal-hydraulic characteristics of the LBE with a high thermal conductivity flowing in the triangular fuel bundle assembly with grid spacers. Subchannel and computational fluid dynamics (CFD) code packages were employed to analyze the thermal-hydraulic phenomenon. The details of the thermal-hydraulic parameters are presented in Table 4. The maximum coolant flow velocity is 0.355 m/s, far below the flow velocity limitation of 2 m/s. Thus, it is certain that this design satisfies operation requirements.

4.3 Design of reactor coolant system

The reactor coolant system consists of four primary heat exchangers, two main coolant pumps, and other auxiliary equipment. The reactor core is located at the lower part of the main vessel to form an integrated pool structure. Four primary heat exchangers are arranged in the annular cavity between the main vessel and the barrel, and one main pump is connected to each two primary heat exchangers. The main composition and flow chart of the reactor coolant system are displayed in Fig. 3.

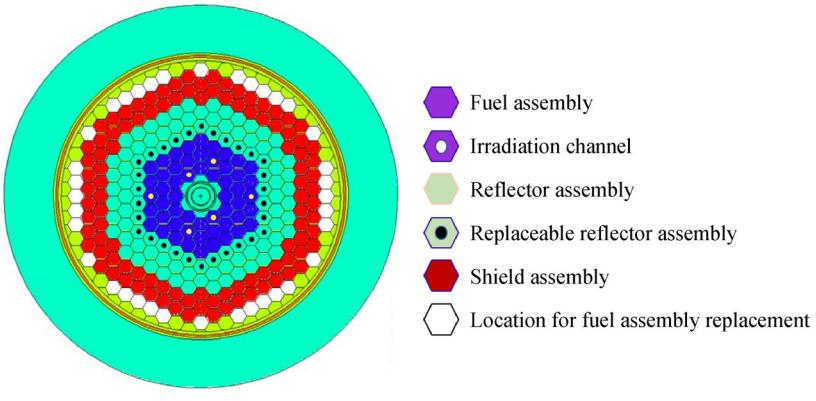

Fig. 4 Layout of subcritical reactor core of CiADS.

Table 3 Core design specifications of CiADS

Item	Value
Reactor thermal power/MW	9.76
Number of fuel assemblies	52
Assembly pitch/mm	181
Active height/mm	1000
Average linear power/(W·cm^{-1})	1885.0
Fuel pin pitch/mm	13.4
Total fuel charge/kg	3880

4.3.1 Main heat exchanger

The primary heat exchanger is the c-type tube heat exchanger, composed of the shell, the tube bundle, the end cover, and the tube sheet. The material is 316L. The secondary inlet header and the secondary outlet header are formed between the tube sheet and the diaphragm. The primary outlet header is installed in the space under the tube bundle.

The inlet and outlet pipes of the secondary circuit are connected to the outlet header at the secondary side and the inlet header at the secondary side by inserting the end cover. A steel plate rolling plate welds the shell, and the support plate is installed on the tube bundle. The shell opening forms the coolant inlet of the primary circuit, and the outlet opening is located at the lower part of the shell. The coolant flows through the chamber between the shell and the tube bundle, as depicted in Fig. 6. The main design parameters are given in Table 5.

4.3.2 Main pump

The function of the main pump is to provide power for the forced circulation of the LBE coolant in the primary circuit. According to the characteristics of flow, system resistance, and installation layout, the main pump adopts a vertical mechanical pump, as shown in Fig. 7. The coolant cooled by the primary heat exchanger enters the main pump from the upper part. It flows to the annular cold pool after being pressurized by the impeller, which provides the pressure head for the circulation of the coolant of the primary circuit. The motor and the shaft are connected by coupling. The design parameters of the main pump are shown in Table 6.

5 Research progress and plan of CiADS subcritical reactor

During 2011–2016, many vital technologies were studied and many achievements were made, as mentioned in Section 2, supported by the ADS Pilot Project [43]. The comprehensive LBE thermal-hydraulic facility, zero-power facility, material synergistic effect of LBE corrosion, and irradiation test facility are established for the LBE reactor research. These scientific infrastructures made an excellent contribution to the LBE reactor research for the ADS technology. However, even though many efforts have been devoted to the CiADS technology, much more

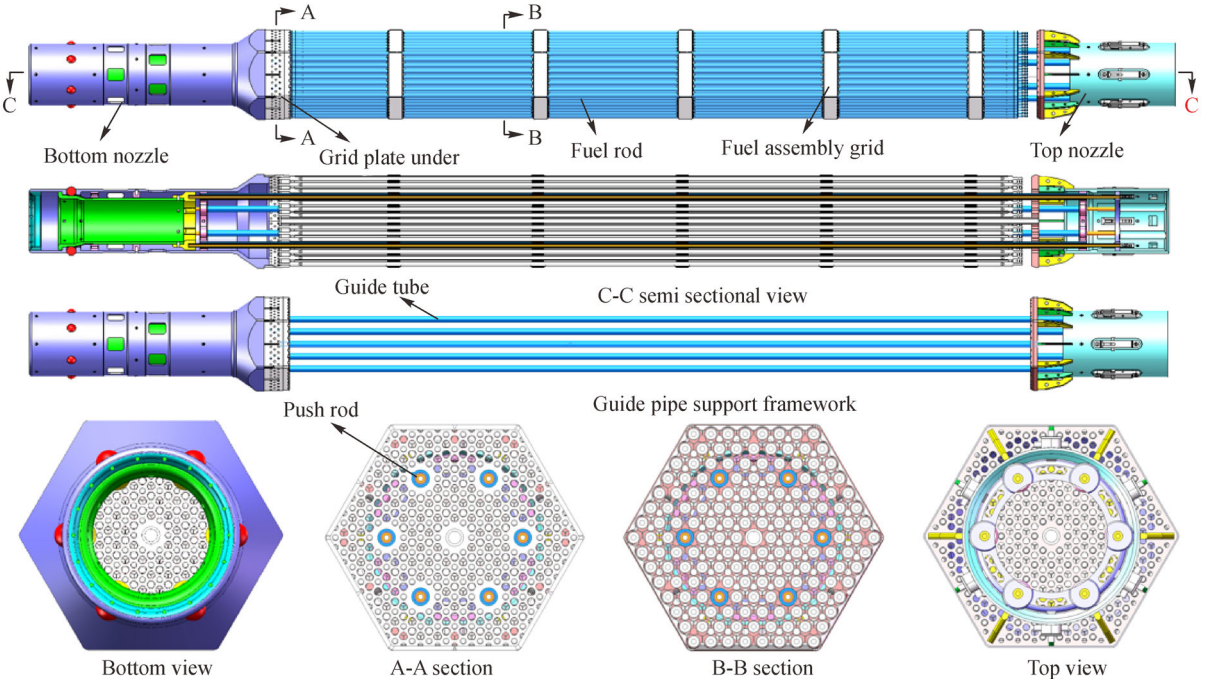

Fig. 5 Layout of fuel assembly of CiADS reactor.

Table 4 Main thermal-hydraulic parameters of subcritical reactor

Item	Value
Inlet average temperature/°C	280
Core temperature difference/°C	100
Outlet average temperature/°C	380
Core total mass flowrate/(kg·s^{-1})	672
Core effective mass flowrate/(kg·s^{-1})	645
Average coolant flow velocity/(m·s^{-1})	0.316
Maximum coolant flow velocity/(m·s^{-1})	0.355
Maximum temperature of fuel centerline/°C	534.29
Maximum temperature of clad outer surface/°C	460.02
Maximum coolant temperature/°C	456.45
Main vessel pressure drop/MPa	0.0087
Core pressure drop/MPa	0.0030
Primary heat exchanger pressure drop/MPa	0.0526

research and development work to support the construction and verification of the CiADS-LBE reactor are still needed. The future research led by IMPCAS will focus on the design software development, experimental validation, nuclear safety verification, and integrated system performance test.

5.1 Development progress and plan for design software of CiADS reactor

5.1.1 Neutron transport program — CAD-PSFO

A geometric description program named CAD-PSFO, which can directly transform the CAD model into the Monte Carlo method, was developed for neutron transport calculation. The ray tracing technology is adopted in the CAD-PSFO program principle, and then the geometric model of boundary representation is analyzed into the model structure of the construction entity [44]. At present, the interface coupling between the "CAD-PSFO and OpenMC" program and the "CAD-PSFO and MCNP" program has been realized, respectively [45,46]. The conversion algorithm and parallel computing for the module structure without data exchange will be developed and verified in the future.

5.1.2 Burnup analysis program — OMCB

For the CiADS subcritical reactor, a calculating program named OMCB of the burnup chain of heavy elements with the coupled Monte Carlo method was developed. In principle, the scanning solution mode deals with the failure problem of the same transfer section in the Bateman equation. The burnup process is solved by the iterative method of prediction correction [47]. At present, the interface coupling design of the OMCB program and OpenMC Monte Carlo program was completed [48,49]. The next step is to develop an accelerated parallel computing method for relatively independent burnup zones and further verify its reliability in engineering design.

5.1.3 Subchannel analysis program — LFR-Sub

Due to the complexity of the flow and heat transfer phenomena of the LBE, the accurate calculation of the coolant and the cladding temperature of the LBE cooled fuel assembly with a wire spacer or a grid spacer is the focus of the thermal analysis of the LBE cooled fast reactor fuel assembly [50]. Based on the lumped parameter method to solve the conservation equation [51], the subchannel analysis code-named LFR-Sub is being developed. The friction resistance model, the turbulent mixing model, and the heat transfer model of the liquid lead-bismuth in rod bundle fuel assembly will be further analyzed and verified. The calculation flowchart of the subchannel code LFR-Sub is plotted in Fig. 8.

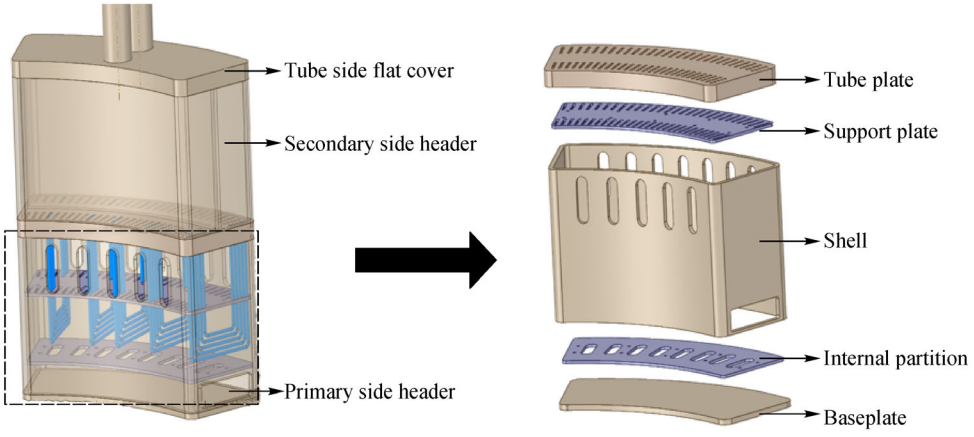

Fig. 6 Schematic diagram of main heat exchanger.

Table 5 Design parameters of main heat exchanger

Item	No.	Parameter name	Value
Global parameters	1	Heat exchanger type	C-tube type
	2	Design pressure/MPa	Atmospheric pressure
	3	Design temperature/°C	400
	4	Test pressure/MPa	Atmospheric pressure
	5	Test temperature/°C	$\geqslant 15$
	6	Operating pressure/MPa	Atmospheric pressure
	7	Operating temperature/°C	380 (Shell side)/230 (Tube side)
	8	Total number of heat exchangers	4
	9	Thermal power/single/MW	2.5
Primary coolant parameters	1	Inlet temperature/°C	380
	2	Outlet temperature/°C	280
	3	Flowrate/single/($kg \cdot s^{-1}$)	172.2
	4	Internal pressure/MPa	Atmospheric pressure + Liquid column static pressure
Secondary side fluid parameters	1	Inlet temperature/°C	220
	2	Outlet temperature/°C	230
	3	Flow rate/single/($kg \cdot s^{-1}$)	114.0
	4	Internal pressure/MPa	Atmospheric pressure

Table 6 Design parameters of the main pump

No.	Parameter name	Value
1	Mass flow rate/($kg \cdot s^{-1}$)	380
2	Head/m	2 (Lead bismuth liquid column)
3	Normal operating pressure/MPa	Atmospheric pressure
4	Normal operating temperature/°C	280
5	Design temperature/°C	400

5.1.4 3D CFD thermal-hydraulic analysis program — 4eqnFoam

It is of significant importance to study the 3D thermal-hydraulic phenomenon of the LBE coolant influencing the security and economic performance of the CiADS subcritical reactor. However, using a CFD code composed of a two-equation turbulence model and a constant turbulent Prandtl number fails to accurately obtain the turbulent heat transfer of the LBE having molecular Prandtl number values in the range of 0.01–0.03 [52,53]. For this purpose, extensive contributions of the turbulent Prandtl number, which can be calculated by a two-equation heat transfer model, were made by researchers [54–62]. Despite the increasing interest in reliable computational tools for LBE fluids to study the turbulent heat transfer in complex industrial applications, commercial codes remain lacking. Thus, a self-compiled four-equation CFD solver named 4eqnFoam is being developed on the open-source CFD package, OpenFOAM [63,64]. The CFD solver, 4eqnFoam, combines a two-equation turbulence model to close the momentum equation and a two-equation heat transfer model to close the energy equation [54–56]. The framework of the four-equation solver, 4eqnFoam, in OpenFOAM is shown in Fig. 9. It can be seen that the 4eqnFoam solver is composed of the velocity equation, UEqn.H, the temperature equation, TEqn.H, the pressure Poisson equation, PEqn.H, the two-equation turbulence model, VEqn.H, and the two-equation heat transfer model, HEqn.H. The executable program, 4eqnFoam, is generated by compiling the wmake command in the Linux terminal. The initial and boundary condition data, the mesh data, the physical property data, the calculation time and output control settings, the discrete format of each differential operator, the algebraic equation solver, and the relaxation factor required by 4eqnfoam are included in the 0 folder, the constant/polyMesh, constant/transportProperties, the system/controlDict, the system/fvSchemes, and the system/fvSolutions.

The future work will address an effort to predict turbulent heat transfer of the LBE flowing in the CiADS-LBE reactor more accurately, based on the CFD solver, i.e.,

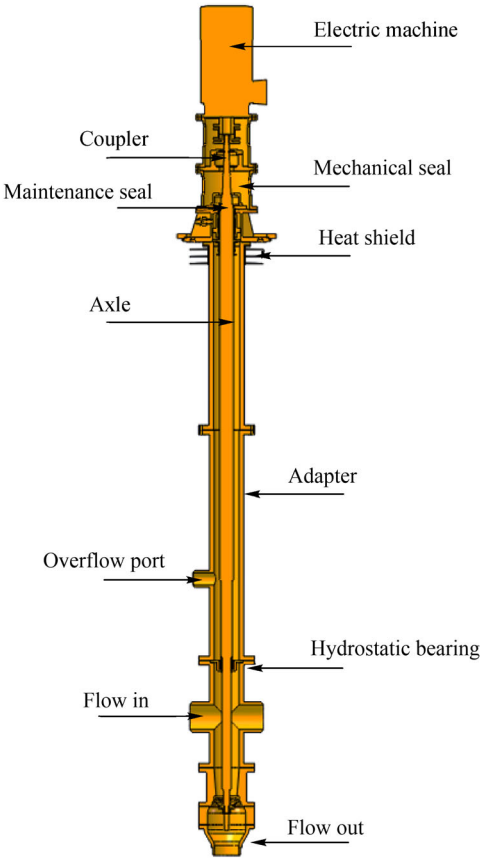

Fig. 7 Structure diagram of main pump.

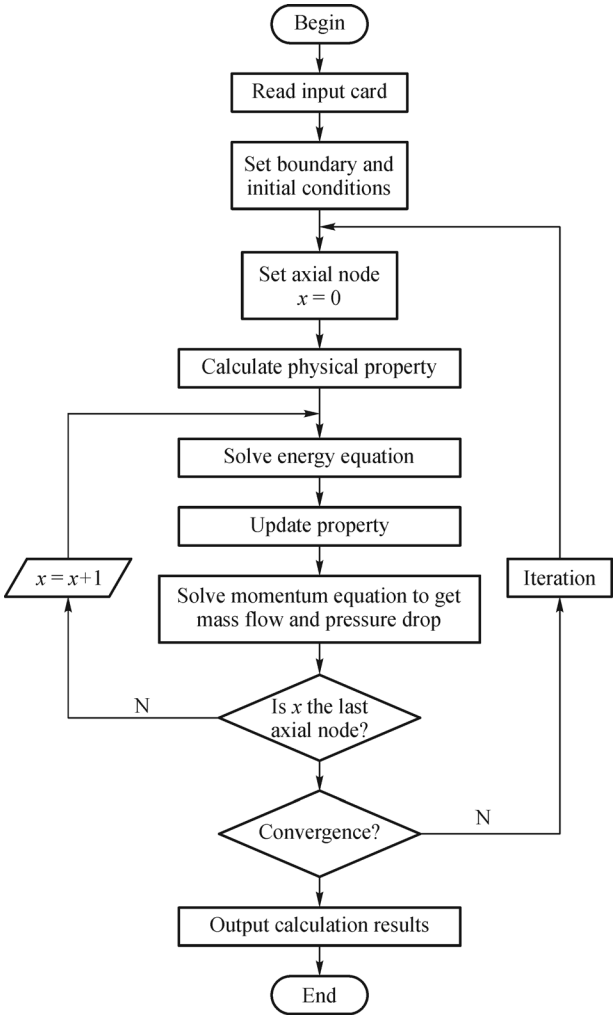

Fig. 8 Calculation flowchart in the sub-channel code LFR-Sub.

4eqnFoam. For the design and application of the LBE subcritical reactor, the next step is to verify and improve the LBE heat transfer program under complex geometry, and develop an algebraic heat flux solver [65] and a second-moment heat flux solver [66].

5.1.5 Analysis program of LBE electromagnetic pump — LFR-ElePump

A design and analysis program for LBE electromagnetic pump named LFR-ElePump is being developed, as shown in Fig. 10. The program is based on the basic mathematical models of electromagnetics, fluid mechanics and heat transfer, and the multi-physics coupling numerical calculation method [67]. The program can determine the geometric parameters, the hydraulic parameters, and the electromagnetic parameters of the electromagnetic pump and conduct the optimization design of the electromagnetic pump structure under certain constraints to make the efficiency, power factor, volume, weight, heat dissipation, and other indicators to achieve the optimal [68]. It can simulate and study the complex behavior of thermal engineering and mechanics for LBE fluids.

5.1.6 System security analysis program

RELAP5 is a transient safety analysis program developed by Idaho National Engineering Laboratory (INEL) for light water reactors for Nuclear Regulatory Commission (NRC). It cannot calculate the power response of the CiADS LBE-cooled subcritical reactor. Thus, based on the Relap5 MOD4.0, the following secondary development work was performed [69,70]: First, the physical parameters and flow and heat transfer model for the simulation analysis of the molten salt medium in the CiADS secondary circuit was implanted. Next, the dynamic analysis model of the point reactor containing the source was invested. Finally, the verification and evaluation of the physical parameters of LBE were completed. Based on the improved RELAP5 with the dynamics calculation capability of the subcritical reactor, the dynamic response characteristics of the CiADS subcritical reactor fuel cladding were obtained under beam transients. In the future, the heat transfer model will be further developed for the fuel assembly and the heat exchanger, the natural convection model in the large space

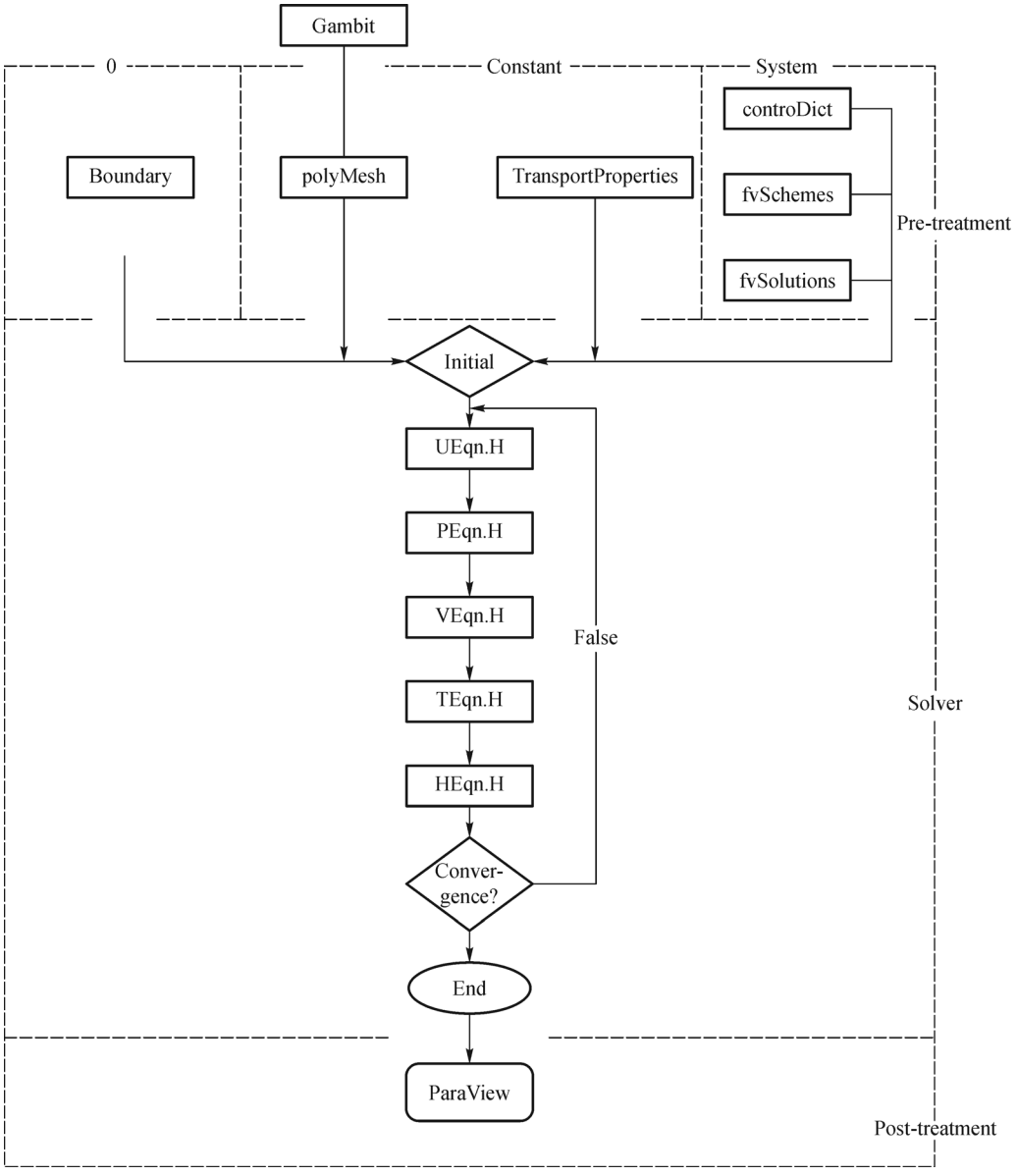

Fig. 9 Framework of four-equation solver, 4eqnFoam, in OpenFOAM.

of pool reactor will be developed and the calculation ability of natural circulation will be verified.

5.1.7 Fuel performance analysis program — FUTURE

For oxide fuel (UO_2), the stainless steel system (the 15-15Ti and the HT-9), and liquid metal coolant (LBE), a fuel analysis tool for nuclear reactor (FUTURE) for oxide fuel rod of the CiADS-LBE reactor is being developed, as shown in Fig. 11. The program can realize thermal analysis, radiation analysis, mechanical analysis, chemical analysis, and residual life analysis of fuel rods [71]. The program FUTURE are characterized by adding liquid LBE corrosion calculation, adding the core-shell chemical interaction kinematic model, and improving the mechanical algorithm based on the geometric nonlinearity under large deformation. Code development and simulation verification of the separation effect of each calculation module has been completed. The full coupling effectiveness of the program will be verified using a fast reactor benchmark and core data in the next step.

5.1.8 Thermal stratification analysis program for LBE — LFR-Buoyancy

A thermal stratification analysis program named LFR-Buoyancy for buoyancy heat transfer of the LBE is being developed, based on the spectral method [72,73], as shown

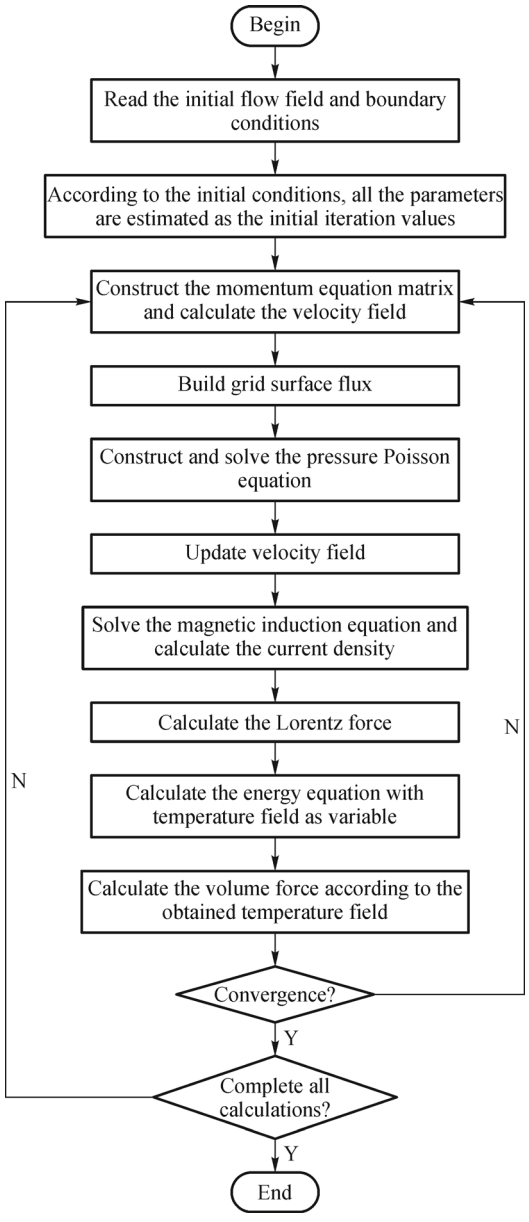

Fig. 10 Framework of analysis program of LBE electromagnetic pump.

in Fig. 12. The buoyancy term has been introduced into the flow and heat transfer equations in the program LFR-Buoyancy. Compared with the finite difference method and the finite element method, the spectral method provides a better solution for some fluid-structure problems which need fine structure. The current program has completed the verification of Rayleigh-Bénard convection. The validity of the code is verified based on the periodic data of a two-dimensional plate with an open boundary. The calculated results were compared with the experimental data in Refs. [74–76]. In the future, the Chebyshev periodic boundary in a two-dimensional problem will be solved so that the code can deal with the issue closer to reality. The code development and debugging of the thermal stratification mechanism will be studied, focusing on developing the solver for turbulence problems.

5.2 Experimental verification for design software

5.2.1 LBE process and material experimental circuit STELA

STELA was initially a loop-type facility for thermal-hydraulic experiments of the LBE coolant. Modification and upgrades are in progress to extend the application of the facility, expected to be completed in 2021. In Fig. 13, after the modification, it is expected that multiple experiments could be conducted on the STELA facility,

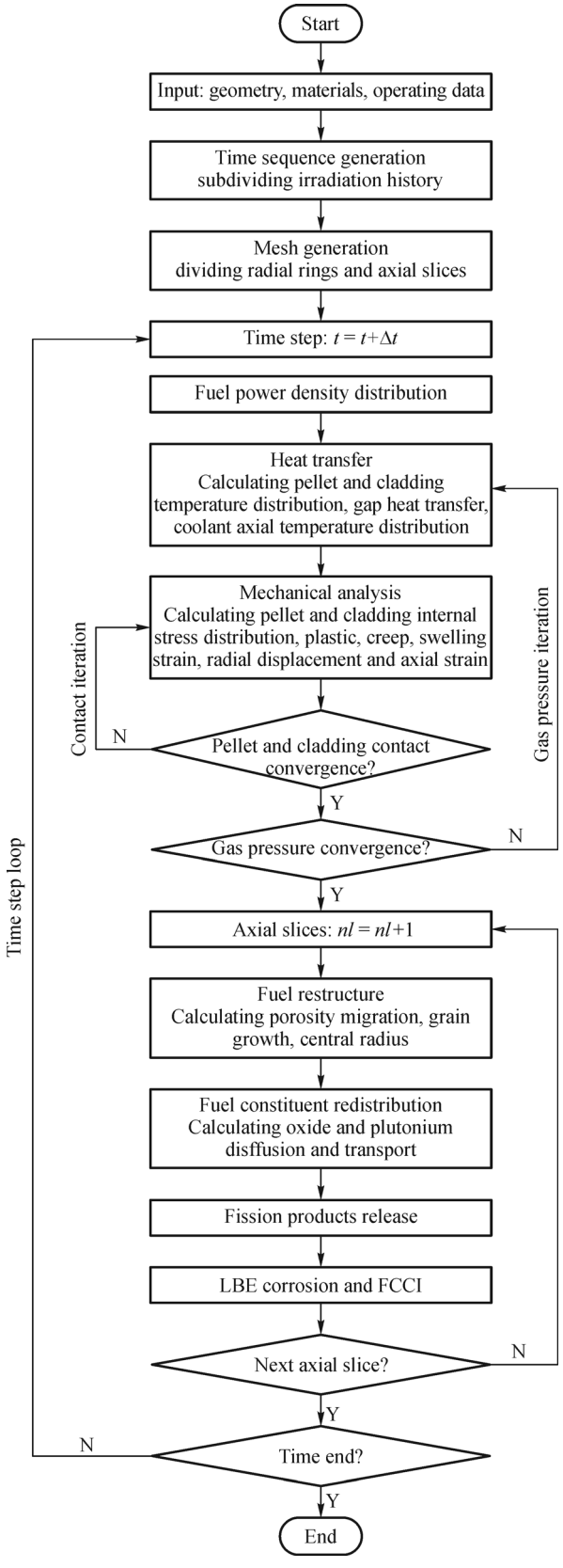

Fig. 11 Framework of fuel performance analysis program FUTURE.

including active oxygen concentration control, cold trap purification technology verification, structural material dynamic corrosion experiment, flowmeter preliminary test, and other experimental activities. At present, the initial design of the testing section and the development of essential equipment have been completed. The basic design parameters of the STELA are shown in Table 7.

5.2.2 Fuel assembly fluid simulation loop

The security and economic performance of nuclear systems will be significantly influenced by the flow characteristics of the fuel assembly. As the positioning component of the fuel assembly of the LFR, the wire-wrap spacer or grid spacer can maintain the fuel pin spacing, reducing the blending and vibration of the fuel pins, enhancing the convective heat transfer. However, the characteristics of high temperature, the opacity, and the corrosiveness of the LBE increase the difficulty of flow and heat transfer experiments in LBE coolant environments [77,78]. The model test results can be applied to the prototype experiment by reasonably designing the test section and selecting the working liquid, based on the dimensional analysis and similarity theory, as long as the Reynolds number similarity is met [79–81]. Thus, a visual fuel assembly fluid simulation loop is built to conduct fluid dynamics experiments of fuel assembly using transparent media such as water based on the proportional modeling method and particle image velocimetry (PIV), as shown in Fig. 14. The loop was divided into a primary loop and a secondary loop. The secondary loop was designed to control the working temperature of the fluid in the primary loop through a water chiller and a heat exchanger. Deionized water was chosen as the working liquid. The operating temperature of the deionized water was 29.0°C±0.5°C. The main parameters in the experimental loop are shown in Table 8.

At present, the periodic pressure distribution of CiADS fuel assembly with wire-wrapped spacers was studied. In that study, a 19-pin wire-wrapped fuel assembly model was designed and manufactured with the same size as the fuel assembly in the CiADS project [82]. In the future, based on the visual hydraulic experimental loop, the pressure drop and turbulence characteristics of the CiADS fuel assembly with wire-wrapped or grid spacers will be further studied under the condition of a large Reynolds number. The comparison of the pressure and velocity distribution between the experimental data and the CFD results will be made to evaluate the applicability of turbulence models. These results will improve the security and the economic performance of the CiADS LBE-cooled subcritical reactor.

5.2.3 Lead bismuth calibration bench

The calibration bench of the LBE coolant is a unique bench

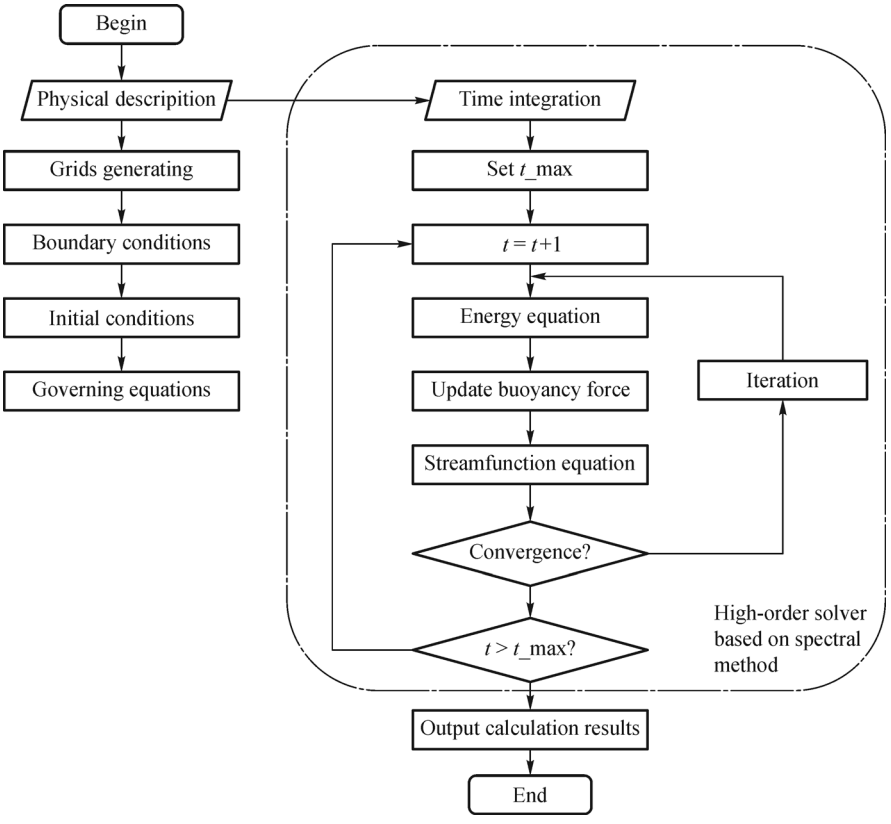

Fig. 12 Framework of thermal stratification analysis program.

for calibrating the flowmeter, level gauge, and circulating pump in the LBE environment. At present, the bench function and loop flow design was completed, as shown in Fig. 15. The critical equipment and technology are being studied. The next step is to complete the design and manufacture of the leading equipment and bench. The simplified flowchart of the lead-bismuth calibration bench is shown in Fig. 16. The calibration method is mainly the static mass method. The diameter range of the gauge to be tested is 25–125 mm. The maximum mass flowrate and operating temperatures are 250 kg/s and 300°C, respectively. Different operation modes can be set according to different functional requirements: calibration of flowmeter by utilizing the weighing method, calibration of flowmeter by utilizing the standard gauge method, calibration of the liquid level gauge, and hydraulic characteristic test of a pump. The weighing tank will be heated by radiation transfer. The calibration bench will effectively support the design of the CiADS LBE cooled reactor.

5.2.4 Zero-power facility of lead-based reactors Venus-I and Venus-II

In 2005, China's first ADS fast-thermal coupling subcritical experimental platform Venus-I was established successfully by the China Institute of Atomic Energy (CIAE) [83], as shown in Fig. 17 [84]. The central region of Venus-I is the fast neutron region, which uses natural uranium as fuel and aluminum as matrix material. Outside the central region is the thermal neutron region, which uses 3% enrichment uranium fuel and polyethylene as matrix material. External neutrons are provided by the ^{252}Cf source or the deuterium-tritium fusion reaction in the high-pressure multiplier to drive the starting force. Neutron experiments related to ADS were performed in Venus-I subcritical facility. The common reactivity measurement methods, such as the jump source method [85], the improved source multiplication method [86], were verified. The critical parameters of the core, the fission rate of the fuel element, the relative distribution of neutron flux density, and the transmutation rate [87] were also measured.

The lead-based critical/subcritical dual-mode operation zero-power facility for ADS research, i.e., Venus-II, achieved the first criticality in December 2016 with the joint efforts of the CIAE and the IMPCAS [88]. The schematic diagram of Venus-II is shown in Fig. 18. The experimental facility consists of a light water core and lead metal core. The light water reactor core is loaded with 20% U_3O_8 fuel. The core structure is simple and belongs to the benchmark device, which is suitable for verifying the accuracy of the physical model, the program calculation, and the nuclear database. The lead metal core is loaded with 20% and 90% enriched U_3O_8 fuel. Lead is used as the

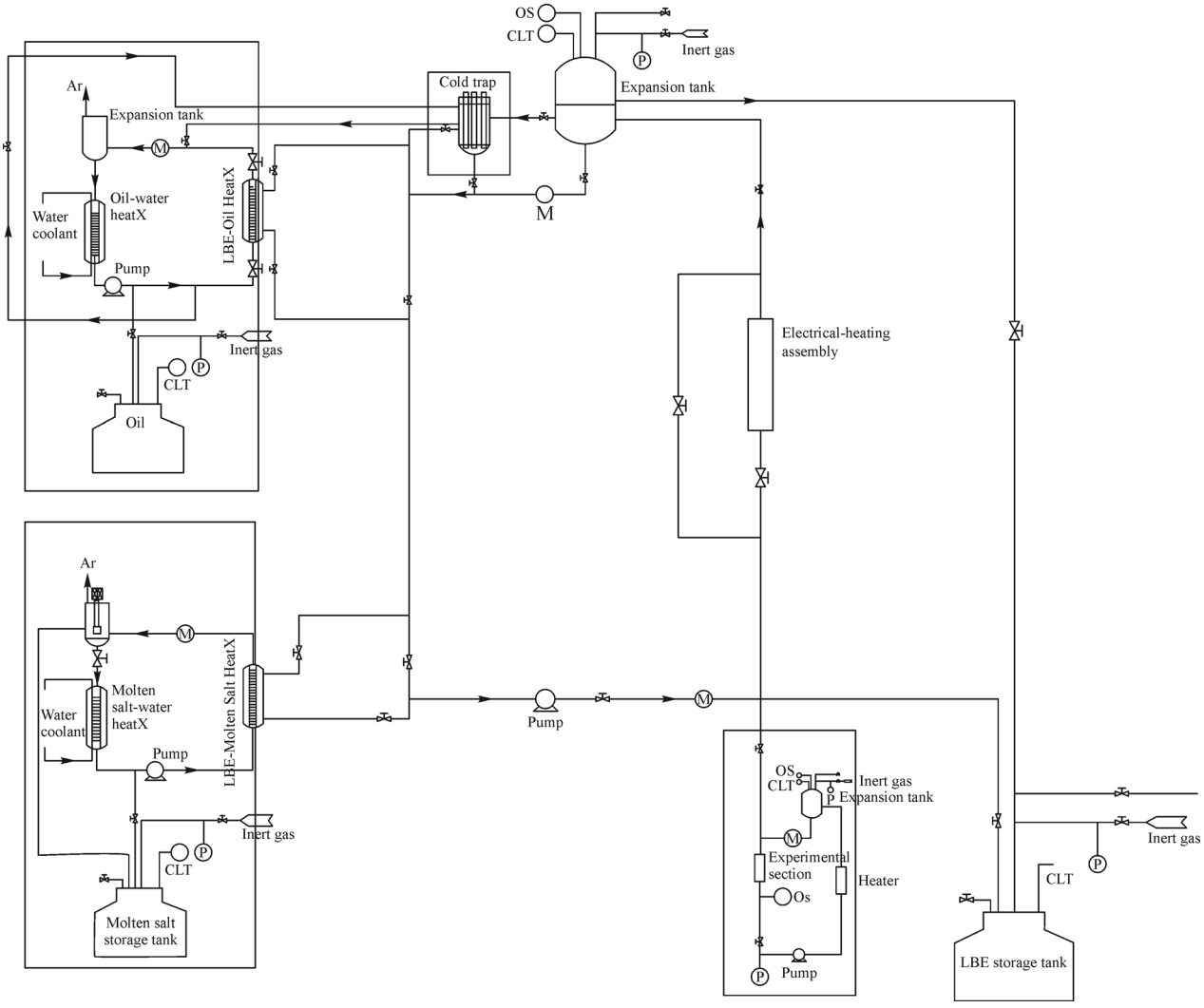

Fig. 13 Diagram of LBE process and material experimental circuit STELA.

Table 7 Main design parameters of STELA

No.	Parameter	Value
1	Length/m	8.0
2	Width/m	6.0
3	Height/m	7.0
4	Coolant	LBE
5	Oxygen control	Cover gas
6	Design pressure/MPa	0.4
7	Loop material	SS 316L
8	Tube size/mm	50(2” Sch80)
9	Total power/kW	500
10	Heat exchanger capacity/kW	500
11	Flow rate/($m^3 \cdot h^{-1}$)	0–15.8
12	Maximum operating temperature/°C	450

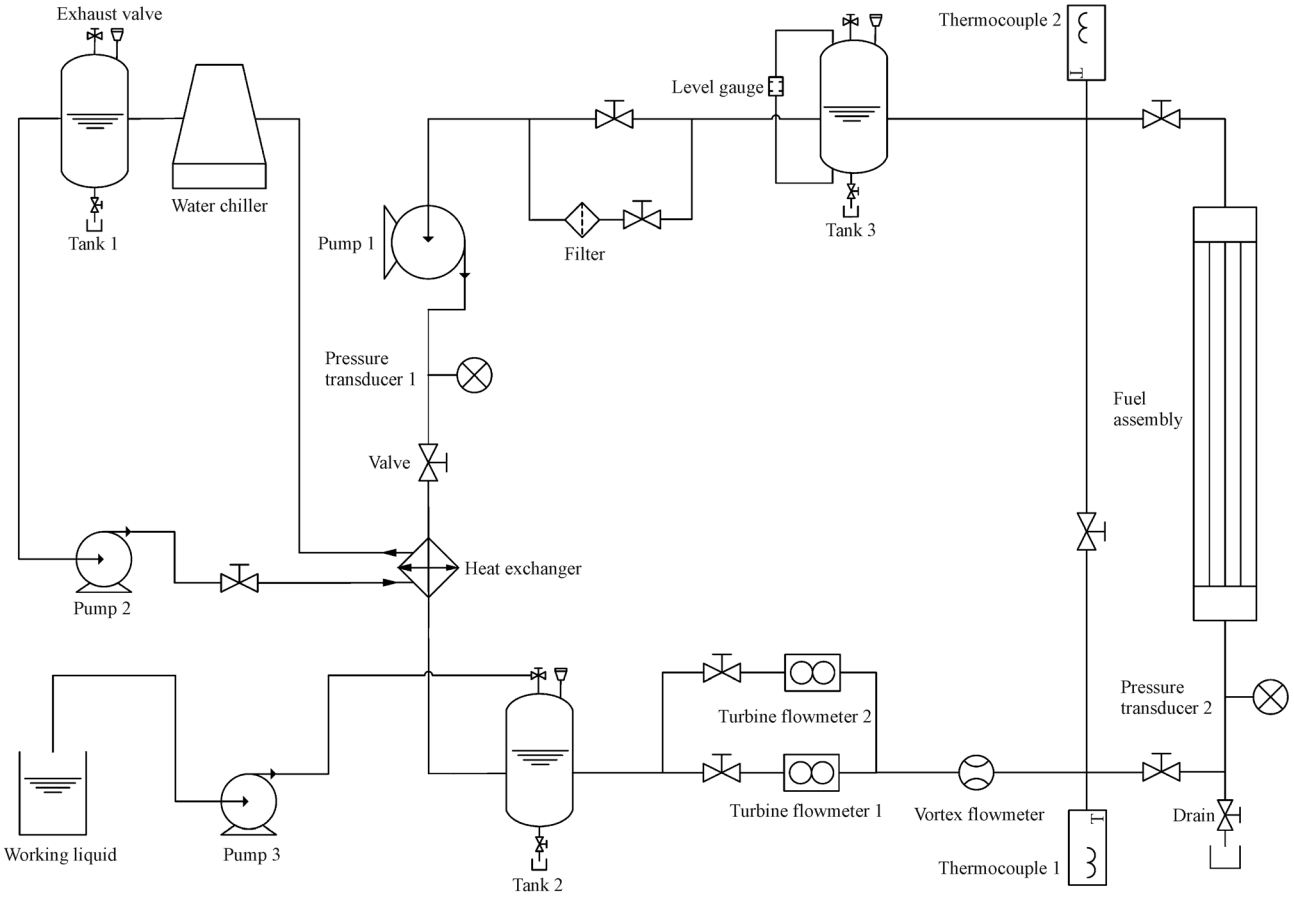

Fig. 14 Diagram of fuel assembly fluid simulation laboratory.

Table 8 Main parameters of experimental loop

Item	Parameter
Main pump	Maximum flow: 40 m^3/h, head: 29 m
Heat exchanger	Type: shell-and-tube, material: 316L
Turbine flowmeter	Range: 1.5–15 m^3/h, accuracy: 0.5%
Turbine flowmeter	Range: 0.4–40 m^3/h, accuracy: 0.5%
TS110 gauge pressure transducer	Range: −100U–100 kPa, accuracy: 0.25%
TS301 differential pressure transducer	Range: –10–10 kPa, accuracy: 0.15%
Particle image velocimetry system	TSI

medium between the fuel and graphite, and polyethylene is used as the reflector materials. The fast region is close to the neutron energy spectrum of ADS, suitable for evaluating the neutronic coupling characteristics between the reactor and the target. Based on the Venus-II, experimental studies of target reactivity value measurement [89,90], reactor dynamic parameters measurement [91], neutron flux, neutron energy spectrum [92], and fission rate [93] were performed. These experimental data, combined with a deterministic program, Monte Carlo program, and various cross-section libraries, were used for a large number of simulation analyses to verify the reliability of experimental measurement and simulation results [94–99].

Further experiments based on Venus-I and Venus-II will be conducted to develop and improve the software of the CiADS subcritical reactor and the measurement method.

5.2.5 LBE corrosion experiment bench

The liquid heavy metal coolant LBE is highly corrosive to traditional structural materials. The corrosion behavior of

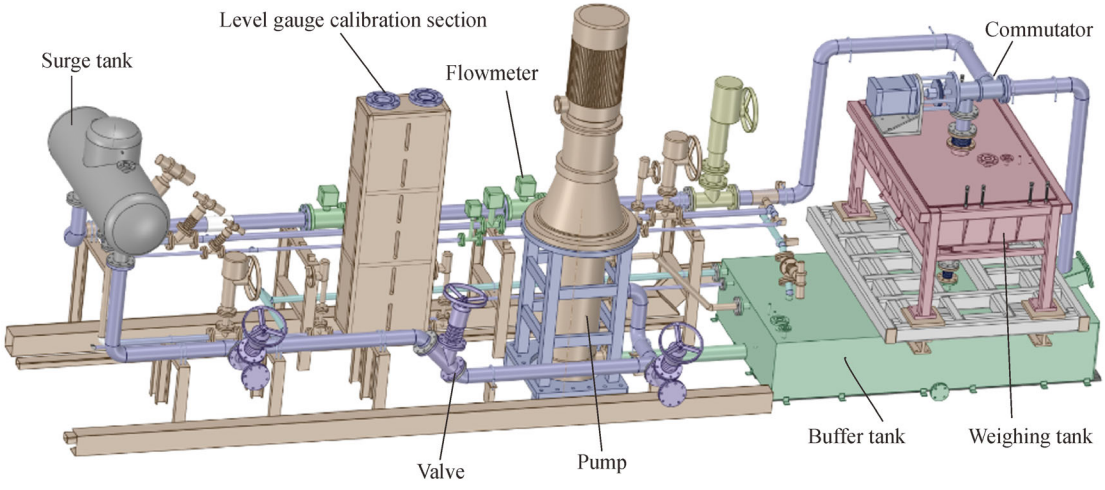

Fig. 15 Conceptual diagram of LBE calibration bench.

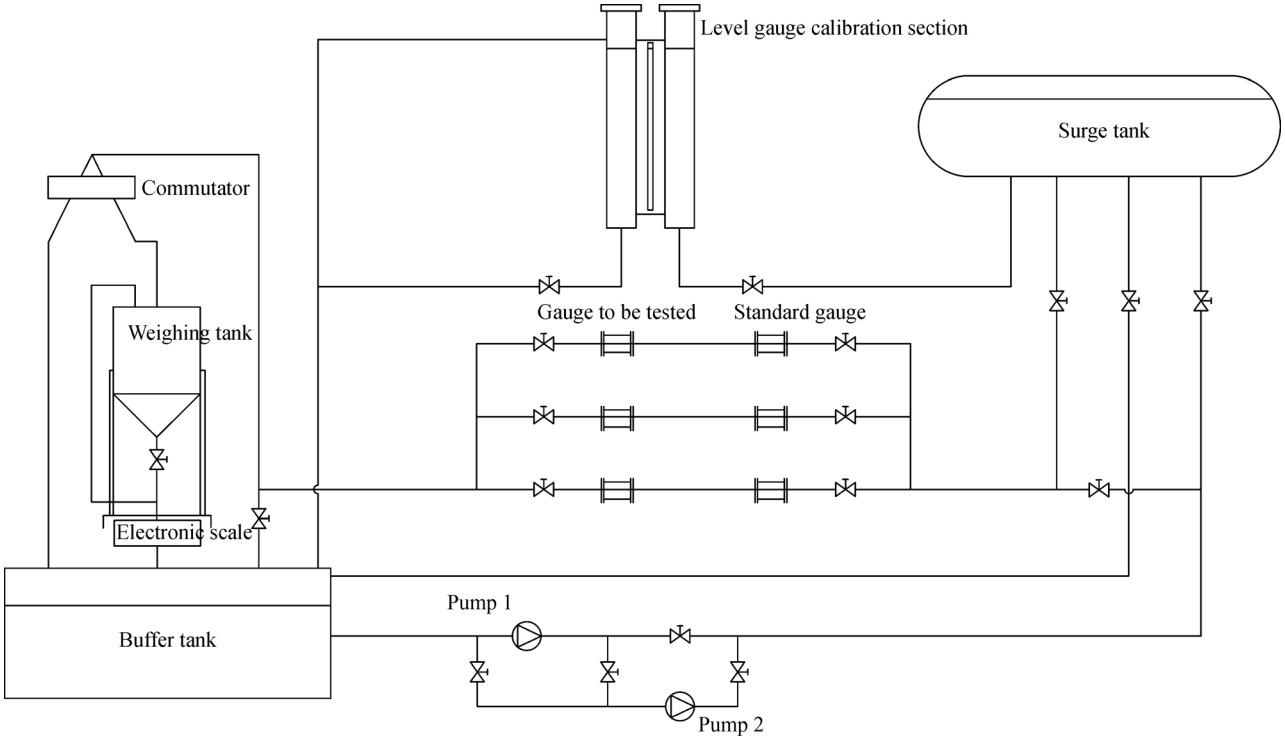

Fig. 16 Simplified flowchart of lead bismuth calibration bench.

stainless steel was qualitatively and quantitatively analyzed and described by theory combining with experiment [100–103]. To study the corrosion behavior of LBE on the structural materials in the CiADS LBE-cooled subcritical reactor, some high temperature static and cooperative corrosion equipment is established under the leadership of IMPCAS, such as the ion irradiation/LBE corrosion synergistic facility, the oxygen controlled liquid LBE corrosion facility, and the oxygen controlled liquid LBE experimental circuit. Figure 19 shows a schematic of the oxygen control LBE corrosion device. As shown in Table 9, the radiation experiment is being conducted. The parameters of the LBE corrosion experiment being performed are shown in Table 10. Ferritic, martensitic steels (SIMP and T91), and austenitic steels (316L and 15-15Ti) were selected as irradiation and corrosion test materials.

In the future, collaborative experiments of stress, corrosion, and radiation should be conducted to study the influence of stress and radiation on LBE corrosion. More

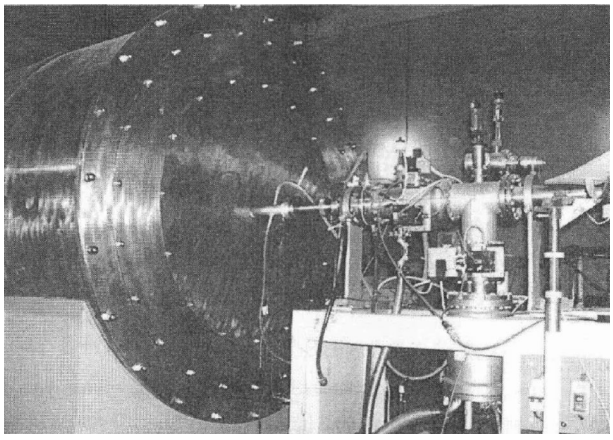

Fig. 17 Schematic diagram of the zero-power facility Venus-I.

Fig. 18 Schematic diagram of zero-power facility Venus-II.

Fig. 19 Schematic diagram of oxygen control LBE corrosion device.

realistic simulations of the corrosion of structural materials in the reactor environment can provide a reliable technical support for the future CiADS project.

5.3 Nuclear safety verification and integrated system performance test

5.3.1 Small integrated verification facility for CiADS

To support the design and construction of the CiADS

Table 9 Main parameters of LBE radiation experiment

Irradiated ion	Temperature/°C	Materials	Irradiation dose point
246.8 MeV Ar^{12+}	350	SIMP	0.2/0.6 dpa
280 MeV Fe^{16+}	350	SIMP	0.2/0.6 dpa
3.5 MeV Fe^{13+}	20	316L/15-15Ti	0.01/0.1/0.01/10 dpa
3.5 MeV Fe^{13+}	350	316L/15-15Ti	0.01/0.1/0.01/10 dpa
3.5 MeV Fe^{13+}	450	316L/15-15Ti	0.01/0.1/0.01/10 dpa
3.5 MeV Fe^{13+}	550	316L/15-15Ti	0.01/0.1/0.01/10 dpa

Table 10 Main parameters of LBE corrosion experiment

Corrosion mode	Temperature/°C	Materials	Corrosion time
Static state	450	15-15Ti/316L	500/1000/2000/4000/6000/8000 h
	550	SIMP/T91/15-15Ti/316L	500/1000/2000/4000/6000/10000 h
After helium ion irradiation	350	SIMP	4000 h
After helium ion irradiation	350	SIMP/T91	2000 h
Synergistic effect	350	SIMP	92h(1.36dpa)/135h(4.8dpa)/295h(13.7dpa)

project, a small integrated verification facility for the CiADS with a total power of 1 MW is designed and built for the thermal-hydraulic test of the fuel assembly, spallation target, core scaling, and leading equipment in the reactor core. The non-nuclear integrated verification facility is a pool-type verification facility based on the CiADS design scheme, which is used to verify the reactor core and critical equipment of the CiADS. At present, the facility has entered the design stage, as shown in Fig. 20. The small integrated verification facility for the CiADS is expected to be completed and used in December 2021.

5.3.2 Comprehensive experimental circuit of LBE

The experimental circuit of LBE mainly serves for the thermal-hydraulic test of the fuel assembly, the calibration and verification of key instruments, the principle verification of essential equipment, and the experimental verification of oxygen-controlled purification. It also aims to accumulate operation and maintenance experience of large and medium-sized liquid LBE circuits. At present, the design process of the experimental circuit has been completed, as shown in Fig. 21. The system is mainly composed of the primary circuit, the secondary circuit, the test section of fuel rod cluster assembly, the pump test section, the flowmeter test section, the oxygen control purification system, the flowmeter calibration system, the molten material tank, the storage tank, the buffer tank, the gas system, and the instrument control system.

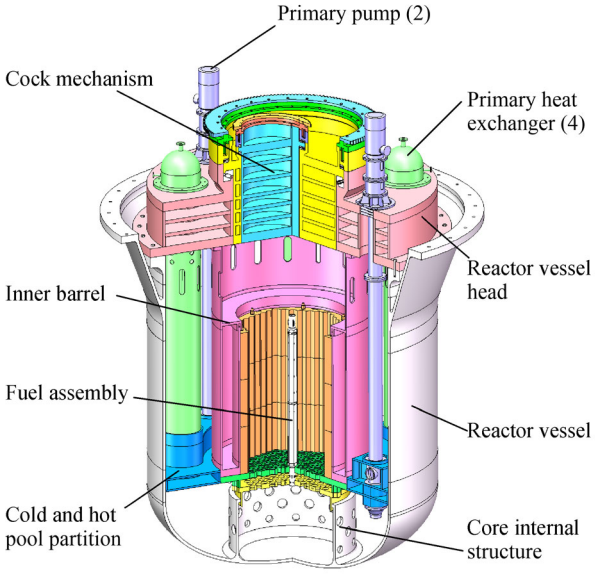

Fig. 20 Conceptual diagram of integrated verification facility of CiADS.

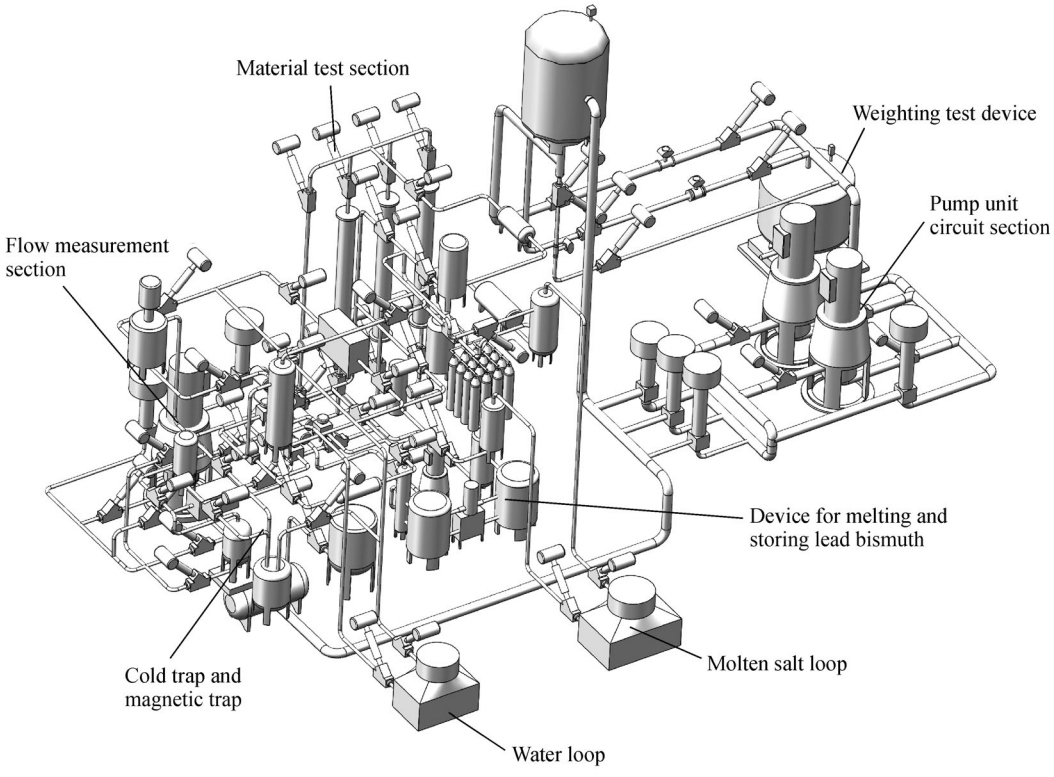

Fig. 21 Conceptual diagram of comprehensive experimental circuit for LBE coolant.

6 Conclusions

Significant progress has been made in China's ADS development in the past decade when China started studying the ADS technology in the mid-1990s. With successful construction and operation of the superconducting proton linac, the VENUS-II facility, and comprehensive experimental facilities for LBE coolant, China plays a pivotal role for advanced steady-state operation toward the next step ADS project. The CAS has made a clear roadmap toward the application of the ADS program in China. The CiADS project for accelerator-driven transmutation verification research is important in the first stage of the ADS technology development. The CiADS project with a total power of 10 MW was approved in 2018 by the Chinese government to start construction in Huizhou, Guangdong province, and is expected to be completed in 2024. The concept design of the CiADS has been completed, and small-scale R&D started five years ago is in progress.

The subcritical reactor is an important part of the whole CiADS. Currently, the pool-type LBE-cooled fast reactor is selected as the preferred reactor type for the CiADS subcritical reactor. Fifty-two fuel assemblies with grid spacers will provide about 9.76 MW of thermal power. To avoid the risk of HXTR, molten salt is used to cool the secondary loop to take away the core heat.

At present, the preliminary design of the CiADS subcritical reactor-based on a pool structure with LBE and molten salt cooling has been completed. It has entered the stage of building an equipment prototype. Detailed engineering designs led by IMPCAS are being conducted to fill the gaps in the construction and operation of CiADS subcritical reactors. Simulation software, such as the neutronics analysis program, the core burnup calculation program, the three-dimensional thermal-hydraulic analysis program for the LBE coolant, the system safety analysis program, the fuel performance analysis program, is being developed to support the optimization design of the CiADS subcritical reactor. Many experiments are being performed based on the experimental platforms, such as the STELA, the LBE coolant calibration platform, the fluid simulation laboratory, the Venus-I, and the Venus-II, to provide reliable verification data for software development. To accumulate construction and operation experience for the CiADS subcritical reactor, a small integrated verification facility and a comprehensive experimental circuit of LBE are being designed and built.

It is expected that the relevant data and design concept presented in this paper can provide some support for the LBE-cooled subcritical reactor design of the ADS technology.

Acknowledgements This work was supported by the Special Fund of Shanghai Municipal Economic and Informatization Commission (GYQJ-2018-2-02).

References

1. Wang C, Engels A, Wang Z. Overview of research on China's transition to low-carbon development: the role of cities, technologies, industries and the energy system. Renewable & Sustainable Energy Reviews, 2018, 81: 1350–1364
2. Chen Y, Martin G, Chabert C, et al. Prospects in China for nuclear development up to 2050. Progress in Nuclear Energy, 2018, 103: 81–90
3. Andriamonje S, Angelopoulos A, Apostolakis A, et al. Experimental determination of the energy generated in nuclear cascades by a high energy beam. Physics Letters [Part B], 1995, 348(3–4): 697–709
4. Rubbia C, Rubio J A, Buono S, et al. Conceptual design of a fast neutron operated high power energy amplifier. Technical Reports, CERN-AT-95-44 ET, 1995
5. NEA-OECD. Physics and Safety of Transmutation Systems: A Status Report. Paris: NEA-OCED, 2006
6. Zhan W L, Xu H S. Advanced fission energy program–ADS transmutation system. Bulletin of the Chinese Academy of Sciences, 2012, 27(3): 375–381 (in Chinese)
7. Mueller A C. Prospects for transmutation of nuclear waste and associated proton accelerator technology. The European Physical Journal Special Topics, 2009, 176(1): 179–191
8. Salvatores M, Slessarev I, Uematsu M. A global physics approach to transmutation of radioactive nuclei. Nuclear Science and Engineering, 1994, 116(1): 1–18
9. Bowman C D, Arthur E D, Lisowski P W, et al. Nuclear energy generation and waste transmutation using an accelerator-driven intense thermal neutron source. Nuclear Instruments & Methods in Physics Research, Section A, Accelerators, Spectrometers, Detectors and Associated Equipment, 1992, 320(1–2): 336–367
10. Abderrahim H A, Kupschus P, Malambu E, et al. MYRRHA: a multipurpose accelerator driven system for research & development. Nuclear Instruments & Methods in Physics Research, Section A, Accelerators, Spectrometers, Detectors and Associated Equipment, 2001, 463(3): 487–494
11. Mishima K, Unesaki H, Misawa T, et al. Research project on accelerator-driven subcritical system using FFAG aaccelerator and Kyoto University critical assembly. Journal of Nuclear Science and Technology, 2007, 44(3): 499–503
12. Ishida S, Sekimoto H. Applicability of dynamic programming to the accelerator-driven system (ADS) fuel cycle shuffling scheme for minor actinide (MA) transmutation. Annals of Nuclear Energy, 2010, 37(3): 406–411
13. Sasa T, Tsujimoto K, Takizuka T, et al. Code development for the design study of the OMEGA Program accelerator-driven transmutation systems. Nuclear Instruments & Methods in Physics Research, Section A, Accelerators, Spectrometers, Detectors and Associated Equipment, 2001, 463(3): 495–504
14. Kurata Y, Takizuka T, Osugi T, et al. The accelerator driven system strategy in Japan. Journal of Nuclear Materials, 2002, 301 (1): 1–7
15. Saito S, Tsujimoto K, Kikuchi K, et al. Design optimization of ADS plant proposed by JAERI. Nuclear Instruments & Methods in

Physics Research, Section A, Accelerators, Spectrometers, Detectors and Associated Equipment, 2006, 562(2): 646–649
16. Rubbia C, Aleixandre J, Andriamonje S. A European Roadmap for Developing Accelerator Driven Systems (ADS) for Nuclear Waste Incineration. ENEA Report, 2001
17. Bianchi F, Artioli C, Burn K W, et al. Status and trend of core design activities for heavy metal cooled accelerator driven system. Energy Conversion and Management, 2006, 47(17): 2698–2709
18. Bauer G S, Salvatores M, Heusener G. MEGAPIE, a 1 MW pilot experiment for a liquid metal spallation target. Journal of Nuclear Materials, 2001, 296(1–3): 17–33
19. Groeschel F, Fazio C, Knebel J, et al. The MEGAPIE 1 MW target in support to ADS development: status of R&D and design. Journal of Nuclear Materials, 2004, 335(2): 156–162
20. Sasa T. Research activities for accelerator-driven transmutation system at JAERI. Progress in Nuclear Energy, 2005, 47(1–4): 314–326
21. Tsujimoto K, Sasa T, Nishihara K, et al. Accelerator-driven system for transmutation of high-level waste. Progress in Nuclear Energy, 2000, 37(1–4): 339–344
22. Sasa T, Oigawa H, Tsujimoto K, et al. Research and development on accelerator-driven transmutation system at JAERI. Nuclear Engineering and Design, 2004, 230(1–3): 209–222
23. Park W S, Shin U, Han S J, et al. HYPER (hybrid power extraction reactor): a system for clean nuclear energy. Nuclear Engineering and Design, 2000, 199(1–2): 155–165
24. Gokhale P A, Deokattey S, Kumar V. Accelerator driven systems (ADS) for energy production and waste transmutation: International trends in R&D. Progress in Nuclear Energy, 2006, 48(2): 91–102
25. Maiorino J R, Santos A D, Pereira S A. The utilization of accelerators in subcritical systems for energy generation and nuclear waste transmutation: the world status and a proposal of a national R&D program. Brazilian Journal of Physics, 2003, 33(2): 267–272
26. Mansur L K, Gabriel T A, Haines J R, et al. R&D for the spallation neutron source mercury target. Journal of Nuclear Materials, 2001, 296(1–3): 1–16
27. Abderrahim H A, D'hondt P. MYRRHA: A European experimental ADS for R&D applications status at Mid-2005 and prospective towards implementation. Journal of Nuclear Science and Technology, 2007, 44(3): 491–498
28. Engelen J, Aït Abderrahim H, Baeten P, et al. MYRRHA: preliminary front-end engineering design. International Journal of Hydrogen Energy, 2015, 40(44): 15137–15147
29. Korepanova N, Gu L, Zhang L, et al. Evaluation of displacement cross-section for neutron-irradiated 15-15Ti steel and its swelling behavior in CiADS radiation environment. Annals of Nuclear Energy, 2019, 133: 937–949
30. Huang Y L, Liu L B, Jiang T C, et al. 650 MHz elliptical superconducting RF cavities for CiADS project. Nuclear Instruments and Methods in Physics Research, Section A: Accelerators, Spectrometers, Detectors and Associated Equipment, 2020, 988: 164906
31. Yu R, Gu L, Sheng X, et al. Review of fuel assembly design in lead-based fast reactors and research progress in fuel assembly of China initiative accelerator driven system. International Journal of Energy Research, 2021, 45(8): 11552–11563
32. Xiao G Q, Xu H S, Wang S C. HIAF and CiADS national research facilities: progress and prospect. Nuclear Physics Review, 2017, 34 (3): 275–283 (in Chinese)
33. Xu Y C, Kang F L, Sheng X Y. Study on the development of accelerator driven system (ADS) and its spallation target. Nuclear Science and Techniques, 2016, 04(3): 88–97 (in Chinese)
34. Dai G X. Nuclear power station driven by accelerator-auxiliary—a clean nuclear energy source. Nuclear Physics Review, 1996, 13(4): 53–58 (in Chinese)
35. Fang S X, Wang N Y, He D H, et al. Suggestions on accelerator driving sub-critical system (ADS) and sustainable development of nuclear energy. Bulletin of Chinese Academy of Science, 2009, 24 (6): 641–644 (in Chinese)
36. Luo P, Wang S C, Hu Z G, et al. Accelerator driven sub-critical systems—a promising solution for cycling nuclear fuel. Physics (College Park, Md.), 2016, 45(9): 569–577 (in Chinese)
37. Ding D Z. The basic research on physics and technology related to the accelerator driven radioactive clean nuclear power system (ADS). China Basic Science, 2001(1): 15–20 (in Chinese)
38. Zhan W L, Yang L, Yan X S, et al. Accelerator-driven advanced nuclear energy system and its research progress. Atomic Energy Science and Technology, 2019, 53(10): 1809–1815
39. Li J Y, Gu L, Yao C, et al. Neutronic study on a new concept of accelerator driven subcritical system in China. In: 26th International Conference on Nuclear Engineering, London, UK, 2018
40. Li J Y, Gu L, Wang D W, et al. The three dimensional immersive training platform for China initiative accelerator driven subcritical system. In: 27th International Conference on Nuclear Engineering, Ibaraki, Japan, 2019
41. Li J Y, Dai Y, Gu L, et al. Genetic algorithm based temperature control of the dense granular spallation target in China initiative accelerator driven system. Annals of Nuclear Energy, 2021, 154 (2): 108127
42. Wang G. A review of research progress in heat exchanger tube rupture accident of heavy liquid metal cooled reactors. Annals of Nuclear Energy, 2017, 109: 1–8
43. Peng T J, Gu L, Wang D W, et al. Conceptual design of subcritical reactor for Chinese accelerator driven transmutation research facility. Atomic Energy Science and Technology, 2017, 51(12): 2235–2241
44. Shriwise P C, Davis A, Wilson P P H. Leveraging intel's embree ray tracing in the DAGMC Toolkit. Transactions of the American Nuclear Society, 2015, 113(pt.1): 717–720
45. Li J Y, Gu L, Xu H S, et al. FreeCAD based modeling study on MCNPX for accelerator driven system. Progress in Nuclear Energy, 2018, 107: 100–109
46. Li J Y, Gu L, Xu H S, et al. CAD modeling study on FLUKA and OpenMC for accelerator driven system simulation. Annals of Nuclear Energy, 2018, 114: 329–341
47. Seifried J E, Gorman P M, Vujic J L, et al. Accelerated equilibrium core composition search using a new MCNP-based simulator. In: Joint International Conference on Supercomputing in Nuclear Applications + Monte Carlo, Paris, France, 2013
48. Li J Y, Gu L, Yu R, et al. Development and validation of burnup-

transport code system OMCB for accelerator driven system. Nuclear Engineering and Design, 2017, 324: 360–371
49. Li J Y, Gu L, Xu H S, et al. The PyNE-Based burnup analysis method for accelerator-driven subcritical systems. Nuclear Technology, 2021, 207(2): 270–284
50. Moorthi A, Kumar Sharma A, Velusamy K. A review of subchannel thermal hydraulic codes for nuclear reactor core and future directions. Nuclear Engineering and Design, 2018, 332(JUN): 329–344
51. Roelofs F, Gopala V R, Jayaraju S, et al. Review of fuel assembly and pool thermal hydraulics for fast reactors. Nuclear Engineering and Design, 2013, 265: 1205–1222
52. Grötzbach G. Challenges in low-Prandtl number heat transfer simulation and modelling. Nuclear Engineering and Design, 2013, 264: 41–55
53. Kays W M. Turbulent Prandtl number—where are we? ASME Transactions Journal of Heat Transfer, 1994, 116(2): 284–295
54. Manservisi S, Menghini F. A CFD four parameter heat transfer turbulence model for engineering applications in heavy liquid metals. International Journal of Heat and Mass Transfer, 2014, 69 (feb): 312–326
55. Manservisi S, Menghini F. Triangular rod bundle simulations of a CFD k-ε-k_θ-ε_θ heat transfer turbulence model for heavy liquid metals. Nuclear Engineering and Design, 2014, 273: 251–270
56. Manservisi S, Menghini F. CFD simulations in heavy liquid metal flows for square lattice bare rod bundle geometries with a four parameter heat transfer turbulence model. Nuclear Engineering and Design, 2015, 295(DEC): 251–260
57. Cerroni D, Da Vià R, Manservisi S, et al. Numerical validation of a k-ε-k_θ-ε_θ heat transfer turbulence model for heavy liquid metals. Journal of Physics: Conference Series, 2015, 655(1): 012046
58. Cervone A, Chierici A, Chirco L, et al. CFD simulation of turbulent flows over wire-wrapped nuclear reactor bundles using immersed boundary method. Journal of Physics: Conference Series, 2020, 1599(1): 012022
59. Chierici A, Chirco L, Da Vià R, et al. Numerical simulation of a turbulent Lead Bismuth Eutectic flow inside a 19 pin nuclear reactor bundle with a four logarithmic parameter turbulence model. Journal of Physics: Conference Series, 2019, 1224(1): 012030
60. Da Vià R, Manservisi S, Menghini F. A k–Ω–kθ–Ωθ four parameter logarithmic turbulence model for liquid metals. International Journal of Heat and Mass Transfer, 2016, 101(oct): 1030–1041
61. Da Vià R, Giovacchini V, Manservisi SA logarithmic turbulent heat transfer model in applications with liquid metals for Pr = 0.01–0.025. Applied Sciences (Basel, Switzerland), 2020, 10(12): 4337
62. Da Vià R, Manservisi S. Numerical simulation of forced and mixed convection turbulent liquid sodium flow over a vertical backward facing step with a four parameter turbulence model. International Journal of Heat and Mass Transfer, 2019, 135: 591–603
63. Weller H G, Tabor G, Jasak H, et al. A tensorial approach to computational continuum mechanics using object-oriented techniques. Computers in Physics, 1998, 12(6): 620–631
64. Moukalled F, Mangani L, Darwish M. The Finite Volume Method in Computational Fluid Dynamics. Berlin: Springer International Publishing, 2016
65. Shams A, De Santis A, Roelofs F. An overview of the AHFM-NRG formulations for the accurate prediction of turbulent flow and heat transfer in low-Prandtl number flows. Nuclear Engineering and Design, 2019, 355: 110342
66. Carteciano L N, Weinberg D, Müller U. Development and analysis of a turbulence model for buoyant flows. In: 4th World Conference on Experimental Heat Transfer, Fluid Mechanics and Thermodynamics, Bruxelles, Belgium
67. Asada T, Aizawa R, Suzuki T, et al. 3D MHD simulation of pressure drop and fluctuation in electromagnetic pump flow. Mechanical Engineering Journal, 2015, 2(5): 15–00230
68. Araseki H, Kirillov I R, Preslitsky G V, et al. Magnetohydrodynamic instability in annular linear induction pump: Part I. experiment and numerical analysis. Nuclear Engineering and Design, 2004, 227(1): 29–50
69. Zhang Q Y, Gu L, Peng T J, et al. Safety analysis of CiADS subcritical reactor fuel cladding under beam transient. Nuclear Power Engineering, 2018, 39(5): 51–57 (in Chinese)
70. Zhang Q Y, Peng T J, Sheng X, et al. Response characteristics of CiADS subcritical reactor fuel cladding under beam transient. Atomic Energy Science and Technology, 2018, 52(05): 931–936
71. Van Uffelen P, Hales J, Li W, et al. A review of fuel performance modelling. Journal of Nuclear Materials, 2019, 516: 373–412
72. Wu K, Welfert B D, Lopez J M. Complex dynamics in a stratified lid-driven square cavity flow. Journal of Fluid Mechanics, 2018, 855: 43–66
73. Cai T. A semi-implicit spectral method for compressible convection of rotating and density-stratified flows in Cartesian geometry. Journal of Computational Physics, 2016, 310: 342–360
74. Alam M R, Liu Y, Yue D K P. Waves due to an oscillating and translating disturbance in a two-layer density-stratified fluid. Journal of Engineering Mathematics, 2009, 65(2): 179–200
75. Baranowski B, Kawczyński A L. Experimental determination of the critical rayleigh number in electrolyte solutions with concentration polarization. Electrochimica Acta, 1972, 17(4): 695–699
76. Aurnou J M, Olson P L. Experiments on Rayleigh–Bénard convection, magnetoconvection and rotating magnetoconvection in liquid gallium. Journal of Fluid Mechanics, 2001, 430: 283–307
77. Carsten S, Olaf W, Aleksandr S, et al. Corrosion kinetics of Steel T91 in flowing oxygen-containing lead–bismuth eutectic at 450°C. Journal of Nuclear Materials, 2012, 431(1–3): 105–112
78. Ejenstam J, Szakálos P. Long term corrosion resistance of alumina forming austenitic stainless steels in liquid lead. Journal of Nuclear Materials, 2015, 461: 164–170
79. Sedov L I. Similarity and Dimensional Methods in Mechanics. 10th ed. Boca Raton: CRC Press. 1993
80. Su G Y, Gu H Y, Cheng X. Experimental and numerical studies on free surface flow of windowless target. Annals of Nuclear Energy, 2012, 43: 142–149
81. Batchelor G K. The application of the similarity theory of turbulence to atmospheric diffusion. Quarterly Journal of the Royal Meteorological Society, 1950, 76(328): 133–146
82. Fan D J, Peng T J, et al. Periodicity and transversal pressure distribution in a Wire-wrapped 19-Pin fuel assembly. International Journal of Energy Research, 2020, 45(8): 11837–11850

83. Shi Y Q, Xia P, Luo Z L, et al. ADS sub-critical experimental assembly–Venus 1#. Atomic Energy Science and Technology, 2005, 5: 447–450
84. Jiang W. Experimental and simulation study of the coupling neutronic behavior of the reactor and spallation target based on Venus II zero-power device. Dissertation for the Doctoral Degree. Hefei: University of science and Technology of China, 2018 (in Chinese)
85. Zhu Q F, Luo H D, Zhang W, et al. Application of source–Jerk method on Venus 1# sub-critical assembly. Atomic Energy Science and Technology, 2010, 44(05): 567–570
86. Liu F, Shi Y Q, Zhu Q F, et al. Measurement of effective delayed neutron fraction for ADS Venus 1# sub-criticality reactor. Atomic Energy Science and Technology, 2016, 50(08): 1445–1448
87. Cao J, Shi Y Q, Xia P, et al. ADS transmutation research based on Venus 1#. Atomic Energy Science and Technology, 2012, 46(10): 1185–1188
88. Zhu Q F, Zhou Q, Zhang W, et al. ADS Venus-II critical extrapolation experiment. Annual Report of China Institute of Atomic Energy, 2017, (00): 106–107
89. Liu Y, Zhou Q, Zhu Q F, et al. Reactivity measurement of solid spallation target in Venus-II by period method. Atomic Energy Science and Technology, 2018, 52(10): 1769–1773
90. Wan B, Zhou Q, Chen L, et al. Reactivity measurement at Venus-II during control rods drop based on inverse kinetics method. Nuclear Engineering and Design, 2018, 338: 284–289
91. Wan B, Luo H D, Ma F, et al. Subcriticality monitoring for lead-based zero power reactor Venus-II using pulsed neutron source method. Atomic Energy Science and Technology, 2018 52(10): 1762–1768
92. Liu F, Zhang W, Liu Y, et al. ADS Venus II neutron spectrum measurement experiment. Annual Report of China Institute of Atomic Energy, 2017: 111–112
93. Wang F, Zhu Q F, Chen X X, et al. Fission rate distribution research for Venus II fast neutron spectrum zone. Atomic Energy Science and Technology, 2018, 52(1): 107–111
94. Jiang W, Gu L, Zhou Q, et al. Measurement of tungsten reactivity worth on VENUS-II light water reactor and validation of evaluated nuclear data. Progress in Nuclear Energy, 2018, 108: 81–88
95. Gu L, Chen L, Zhou Q, et al. Measurement of tungsten granular target worth on VENUS-II light water reactor and validation of the granular target model. Annals of Nuclear Energy, 2021, 150: 107825
96. Jiang W, Gu L, Zhu Q F, et al. Experimental and simulation study on fuel rod value of VENUS-II light water reactor. Atomic Energy Science and Technology, 2018, 52(09): 1665–1670
97. Zhang L, Yang Y W, Ma F, et al. Deterministic simulation of the static neutronic characteristics for the lead core of VENUS-II facility. Nuclear Engineering and Design, 2019, 353: 110258
98. Jiang W, Gu L, Zhu Q F, et al. Reactivity worth measurement of the lead target on VENUS-II light water reactor and validation of evaluated nuclear data. Annals of Nuclear Energy, 2021, 154: 108106
99. Jiang W, Gu L, Zhang L, et al. Validation of neutron evaluated data based on the experimental reactivity worth of tungsten target in CiADS. EPJ Web Conference, 2020, 225: 04026
100. Zhang J S, Li N. Review of the studies on fundamental issues in LBE corrosion. Journal of Nuclear Materials, 2008, 373(1–3): 351–377
101. Park J J, Butt D P, Beard C A. Review of liquid metal corrosion issues for potential containment materials for liquid lead and lead–bismuth eutectic spallation targets as a neutron source. Nuclear Engineering and Design, 2000, 196(3): 315–325
102. Zhang J S. A review of steel corrosion by liquid lead and lead-bismuth. Corrosion Science, 2009, 51(6): 1207–1227
103. Zhang J, Hosemann P, Maloy S. Models of liquid metal corrosion. Journal of Nuclear Materials, 2010, 404(1): 82–96